Cholesterol Ozonolysis: Kinetics, Mechanism, and Oligomer Products

Matthew A. Dreyfus, Michael P. Tolocka, Scott M. Dodds, John Dykins, and Murray V. Johnston*

Department of Chemistry and Biochemistry, University of Delaware, Newark, Delaware 19716

Received: February 3, 2005; In Final Form: May 19, 2005

Fine particles of cholesterol were reacted with ozone under pseudo-first-order conditions in an aerosol bag reactor. Gas-phase ozone was monitored using an ozone meter. Particle size distribution functions were determined using a scanning mobility particle sizer, which selected particle sizes for introduction into a photoionization aerosol mass spectrometer (PIAMS). PIAMS was used to determine the concentration of cholesterol in the aerosol as a function of reaction time. Dilution corrected rate coefficients were used to calculate the reactive uptake coefficient for ozone onto cholesterol particles as $(2.8 \pm 0.4) \times 10^{-6}$. Uptake was found to be independent of particle diameter for the sizes studied (100 and 200 nm), suggesting that the uptake is surface mediated. The reaction products were also collected on filters and analyzed by electrospray ionization (ESI) mass spectrometry with both direct infusion and liquid chromatography sample introduction. The main primary reaction products contained one, two, or three oxygens added to the cholesterol moiety. Secondary oligomeric products were also observed, consisting of covalently bound dimers and trimers. Tandem mass spectrometry was used to confirm the expected structures of these compounds. The dimers appear to be acyl hydroperoxides, consistent with a previously reported mechanism for the reaction in a nonparticipating solvent. Finally, the magnitude of the uptake coefficient confirms that cholesterol is suitable as a local source tracer for source apportionment of ambient organic aerosol.

Introduction

Organic molecular markers are frequently used as source tracers for primary and secondary organic carbonaceous aerosols in urban and rural environments.[1−4] For molecular markers to be functional, they must meet certain criteria: (1) they must be emitted in large enough amounts to be measurable upon dilution and mixing in the atmosphere, (2) they must be unique to the particular emission source, and (3) reactions should not occur that significantly remove or produce these species between their emission from the source and detection at the measurement site.

Many studies have focused on (a) identifying molecular markers from biomass combustion,[5,6] meat cooking operations,[7] fireplaces,[8] motor vehicle emissions, and other sources,[9−11] and (b) improved technology for making composition resolved measurements.[12−19] Some of the organic compounds that are proposed for use in source apportionment contain a double bond, including cholesterol, a marker for meat cooking operations. The behavior of aerosol phase cholesterol in the atmosphere is unclear. It has long been known that oligomers form from the ozonolysis of alkenes in practical laboratory processes.[20,21] Cholesterol itself is known to form these high molecular weight compounds in nonparticipating solvents and may also form them in the presence of water.[22]

The aim of this study is to understand the reactivity of cholesterol aerosol under nominally dry conditions. The loss of reactant is monitored with a photoionization aerosol mass spectrometer (PIAMS) to determine the magnitude of the uptake coefficient of ozone onto cholesterol particles and to determine the physical mechanism of uptake. Reaction products are identified by electrospray ionization (ESI) in a quadrupole time-of-flight (QTOF) mass spectrometer with both direct infusion and liquid chromatographic sample introduction. Expected product structures are confirmed by tandem mass spectrometry (MSMS).

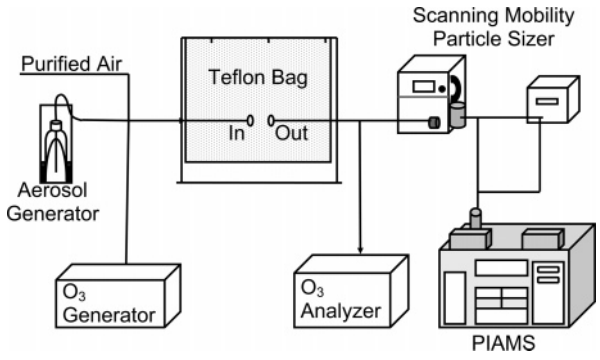

Figure 1. Schematic of experimental setup. Aerosolized cholesterol particles and ozone are produced sequentially and sent into the aerosol chamber. The ozone concentration is measured using the ozone meter; cholesterol particles are size-selected with the DMA and then measured with the PIAMS.

Experimental Section

Experiments were performed with an aerosol bag reactor attached to a photoionization aerosol mass spectrometer[23] (PIAMS) for on-line analysis as shown in Figure 1. Particles were also collected onto a filter for off-line analysis. Cholesterol aerosol was produced using a constant output atomizer (model 3076, TSI, Inc.). This aerosol was generated from a solution of 0.5 g of cholesterol in 1000 mL of ethanol. All generated aerosol was neutralized by a ^{210}Po radioactive static eliminator. A series of flow meters selected a steady flow rate. Ozone was generated

* Corresponding author. Phone: (302) 831-8014. Fax: (302) 831-6335. E-mail: mvj@udel.edu.

10.1021/jp050606f CCC: $30.25
Published on Web 06/22/2005

with a commercially available "Ozone Purification" system (Prozone Inter. PZ6-AIR, Huntsville, AL).

The aerosol chamber is a 500 L bag with Teflon walls and two Swagelok adaptors that function as the inlet and outlet. Prior to each experiment, the bag was flushed with dry clean filtered air for a few hours (RH = 5%). Leftover air in the bag was sampled with a scanning mobility particle sizer (SMPS; TSI, Inc.) to confirm that the background particulate matter level was less than 0.5 $\mu g/m^3$. At the start of an experiment, the bag was filled with purified air until visibly inflated. Next, aerosolized cholesterol (produced from the aforementioned solution with the TSI atomizer) was introduced into the chamber at a set flow rate for a 5-min span. The flow rate was adjusted between 1 and 2 L/min to establish a set concentration of cholesterol in the chamber. The aerosol flow was turned off, and another sample was taken with the SMPS to determine the cholesterol concentration in the chamber. Extra time, between 10 and 20 min, was then allotted to allow the aerosol to diffuse throughout the chamber. Beginning concentrations of cholesterol in the aerosol were on the order of 100−300 $\mu g/m^3$.

Ozone was generated and sent into the chamber for between 1 and 2 min. The ozone concentration was varied, but kept high enough to ensure pseudo-first-order conditions (700−2000 ppb; ≥10-fold molar excess with respect to cholesterol). In all, seven separate experiments were performed using cholesterol and ozone concentrations within the ranges specified above. The ozone concentration was monitored during the experiment using an ozone analyzer (Model 49C, Thermo Electron Corp.), which was connected through the chamber's outlet. Once the desired ozone concentration in the chamber was reached, the inlet was sealed and sampling with PIAMS began. The ozone concentration was monitored during the course of the experiment to ensure that it remained constant. For the reaction times studied here, wall loss of ozone was typically less than 5% of the starting value. No reduction in the ozone concentration due to reaction with cholesterol was observed. Particle and ozone concentration measurements before and during the reaction verified that the reactants were well mixed.

Aerosol exiting the chamber was first size selected with the differential mobility analyzer (DMA model 3080, TSI Inc.). The selected particle size alternated between 100 and 200 nm. For on-line analysis, these particles were sent from the DMA to the PIAMS through conductive tubing. When PIAMS was not in use or when SMPS measurements were being performed, the aerosol stream bypassed the PIAMS and was sent to the condensation particle counter (CPC model 3025a, TSI Inc.).

The PIAMS used for on-line analysis has been discussed in detail previously.[23] Briefly, the aerosol enters the mass spectrometer through an aerodynamic lens assembly, which produces a focused particle beam.[24,25] The particle beam traverses three differential pumping stages and impinges on a probe in the ion source region. After a sufficient particle mass is collected (approximately 1 ng), a pulsed infrared laser irradiates the probe surface. The laser radiation is absorbed by the probe material, and to a lesser extent by the sample itself, to induce a rapid temperature increase (microsecond time scale) at the probe surface. Chemical components in the particles are flash desorbed from the probe surface into the center of the ion source region. About 30 μs after the desorption laser pulse, a second laser fires to ionize the desorbed compounds. Ionization is performed by single photon ionization (SPI) with 10.5 eV photons. The photoionization mass spectrum is obtained with a reflectron time-of-flight mass analyzer that allows the entire mass spectrum to be obtained for each laser pulse.

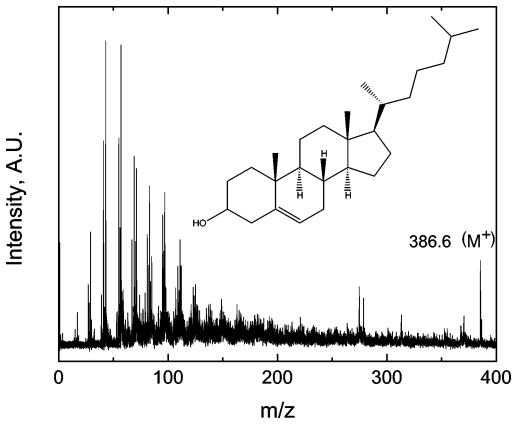

Figure 2. Mass spectrum of 200 nm cholesterol particles (molecular structure shown in inset). This spectrum is an average of 50 individual spectra from the 60 s sample. The amount of mass collected is on the order of 0.5 ng.

To sample aerosol from the bag, the inlet to PIAMS was opened for 60 s. Immediately after sampling, the lasers began pulsing at 10 Hz. Initially 150 spectra were collected; however, as the reaction time increased and the cholesterol concentration decreased, the number of collected spectra was reduced to 70 as this was sufficient to completely desorb the smaller amount of cholesterol deposited on the probe. After the collection of spectra, the desorption laser was fired another 100 times to clean the probe of any residual material. Of the collected spectra, the first 50 were averaged to produce a single, representative spectrum as virtually all sample was desorbed in this time period. The entire data collection process was repeated every few minutes for the duration of the experiment (∼1 h). The experiment was replicated eight times. The relative humidity for each experiment was 5%.

The ability of PIAMS to perform a soft ionization allows for sensitive detection of the cholesterol molecular ion (386 *m*/*z*; $C_{27}H_{46}O$) with minimal fragmentation. Figure 2 shows an example mass spectrum. Integration of the parent ion peak gives a measure of the relative concentration of cholesterol as a function of reaction time.[23] These concentrations subsequently were corrected for aerosol losses to the walls of the bag. The aerosol concentration half-life in the bag due to wall losses is on the order of 90 min.

For off-line analysis, samples were taken from the bag after 30 min of reaction by withdrawing aerosol at 20 Lpm onto pre-extracted 47 mm Teflon impregnated glass fiber filters (type T60A20, Pallflex Products Corp., Putnam, CT). The filters were ultrasonically extracted in 20 mL of solvent. A variety of solvents were used to confirm that no further reaction took place during extraction. The solvents included acetonitrile, methanol, THF:H_2O (50:50 vol %), and methylene chloride. The extracted samples were concentrated to 0.5 mL using a dry stream of nitrogen or centrifuged under vacuum, spiked with 1 mM ammonium acetate in MeOH (50:50 v/v spiking ratio), and then directly infused into an ESI-QTOF mass spectrometer (Micromass API-US QTOF, Beverly, MA). The samples were analyzed by MS and MSMS scans in both positive and negative ion modes. In most cases, 100−200 μL of spiked solution was sufficient for analysis. Filter and solvent blanks were run to test for any background impurities that might have affected the analysis.

Aliquots of sample were also introduced into an LC−MS system (CapLC, Waters, Waltham, MA) with reversed phase separation using a Jupiter 5 C18 (250 × 1 mm) column (Phenomenex, Torrance, CA). The gradient was the same as

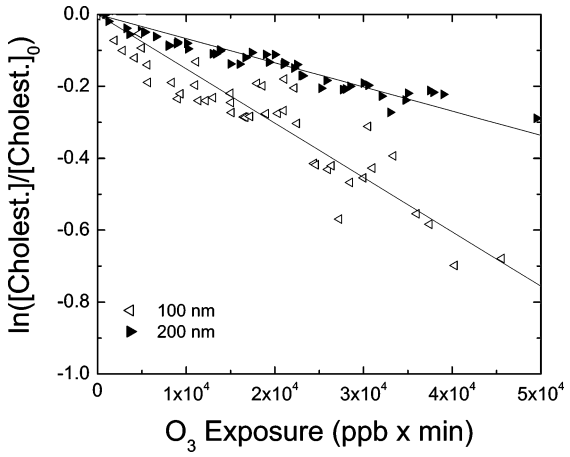

Figure 3. Plot of the logarithm of the normalized cholesterol molecular ion (386 *m*/*z*) signal intensity versus ozone exposure for 100 and 200 nm diameter particles. The data points in these plots are the combined measurements from seven separate experiments with cholesterol concentrations in the aerosol ranging from 100 to 300 μg/m^3 and ozone concentrations ranging from 700 to 2000 ppb. The data point values for each particle size are smoothed by adjacent three-point averaging and then fit with a linear regression to determine the rate coefficients.

described by Pulfer et al.[26] Briefly, solvent A and solvent B start at a 50:50 ratio and ramp to 100% B over 20 min. Solvent B continues for another 20 min for a total of 40 min. Total flow was limited to 40 μL/min. There is an allowance of 10 min for reequilibration before the next run. Solvent A consists of 20:20:60 ratio of acetonitrile, water, and methanol, and solvent B consists of 100% methanol. Both contained 1 mM of ammonium acetate to facilitate ammonium cationization (+18 u) in the positive ion mode and acetate anionization (+59 u) in the negative ion mode. Again, filter and solvent blanks were analyzed.

Eight separate experiments were performed with off-line analysis. A sample blank was obtained for each experiment. Similar mass spectra were obtained from different extracts of the same filter and from different experiments of the same type (e.g., different solvents).

Results and Discussion

Reaction Rate and Mechanism of Uptake. On-line analysis with PIAMS permitted the amount of cholesterol remaining in the aerosol to be measured as a function of exposure to ozone. The reaction mechanism and uptake coefficient obtained from it were determined from the reaction rate and its dependence on the ozone concentration and particle size. Figure 3 shows plots of the logarithm of the normalized cholesterol concentration versus ozone exposure (ozone concentration multiplied by reaction time) for 100 and 200 nm mobility diameter particles. The exposure history for each experiment is different; that is, one time interval at one ozone concentration during one experiment does not exactly coincide with another time interval for another experiment. Because this did not allow the collected data from different experiments to be averaged directly, the data points for each particle size in Figure 3 were smoothed using three-point adjacent averaging. The logarithmic dependence in Figure 3 combined with a reaction rate that is approximately inversely proportional to particle diameter ($k_{100nm}/k_{200nm} = 2.25$) indicates that uptake is dominated by surface interactions.[27−29] It should be noted that while the logarithmic plot in Figure 3 fits the data with higher correlation coefficients ($R^2_{100nm} = 0.93$; $R^2_{200nm} = 0.88$) than a square root concentration dependence ($R^2_{100nm} = 0.86$; $R^2_{200nm} = 0.86$), the precision is not high enough to distinguish the two. A square root dependence would indicate that uptake is limited by reaction within a thin layer near the surface.

TABLE 1: Experimentally Determined Rate Coefficients and Uptake Coefficients for the Reaction of Ozone with Cholesterol Particles

mobility diameter (nm)[a]	k_{II} (cm^3 molecule^{-1} s^{-1})	γ_o
100	$(1.02 \pm 0.15) \times 10^{-17}$	$(2.94 \pm 0.28) \times 10^{-6}$
200	$(4.54 \pm 0.11) \times 10^{-18}$	$(2.64 \pm 0.22) \times 10^{-6}$
ratio (100 nm/200 nm)	2.25	1.11
average		$(2.8 \pm 0.4) \times 10^{-6}$

[a] Spherical particles are assumed. If the particles are not spherical, then substitution of the mobility diameter for the volume equivalent diameter will overestimate the amount of cholesterol in a particle and thereby give an underestimate of the uptake coefficient. For polycrystalline and/or compact aggregate particles commonly found in ambient air, this error is typically less than 5%.[30] The measured rate constants are unaffected by the spherical particle assumption.

The slopes of the lines in Figure 3 give values for k_{II}, the second-order rate coefficients, which are presented in Table 1 for both particle sizes. The initial uptake coefficient, γ_o, or the probability that a reaction will occur upon the collision between a cholesterol particle and ozone, can be expressed in terms of the rate of change of the cholesterol concentration[29] (determined from the change of the integrated parent ion signal at 386 *m*/*z*):[23]

$$\gamma_o = -\frac{\partial[\text{Chol.}]}{\partial t}\frac{2d}{3u[O_3]} = \frac{2k_{II}d[\text{Chol.}]_o}{3u} \qquad (1)$$

where d is the volume equivalent particle diameter (diameter of a spherical particle having the same volume as the actual particles that were analyzed; taken in this work as the mobility diameter), u is the average ozone molecular speed, k_{II} is the second-order rate coefficient from Table 1, and $[\text{Chol.}]_o$ is the condensed phase cholesterol concentration in the original (unreacted) solid. Note that eq 1 does not assume a particular uptake model. Values for γ_o at each particle size are presented in Table 1. This analysis assumes that the particle size does not change as the reaction proceeds (i.e., as cholesterol is oxidized) and that substitution of the mobility diameter for the volume equivalent diameter does not lead to a substantial error. For polycrystalline and/or compact aggregate particles commonly found in ambient air, this error is typically less than 5%.[30]

The uptake coefficient determined in this study of $(2.8 \pm 0.4) \times 10^{-6}$ (average of 100 and 200 nm diameter particles) is smaller by 2 orders of magnitude than that previously reported for liquid alkene surfaces such as oleic and linoleic acid.[28,31] However, for solid frozen surfaces of unsaturated fatty acids,[32] the uptake coefficients were found to be ca. 7×10^{-5}, which are closer to but still larger than the value obtained here for cholesterol. Given the inherent rigidity and steric hindrance of the cholesterol structure relative to a straight chain hydrocarbon and the fact that dry cholesterol particles are solid, this difference does not seem unreasonable.[33]

Product Identification by Off-Line Analysis. While the molecular ion signal intensity decreases with increasing exposure to ozone, no new product ions were observed by PIAMS, in part because the product m/z values exceeded the m/z range analyzed. Instead off-line analysis of collected particles was performed to identify the products. Figure 4 shows the ESI-QTOF mass spectrum of an extract of the aerosol formed from the reaction of cholesterol aerosol and ozone. Note that some cholesterol remains as indicated by peaks at 369 *m*/*z* ($M - OH^+$) and 404 *m*/*z* ($M + NH_4^+$). Ion groupings are observed up to

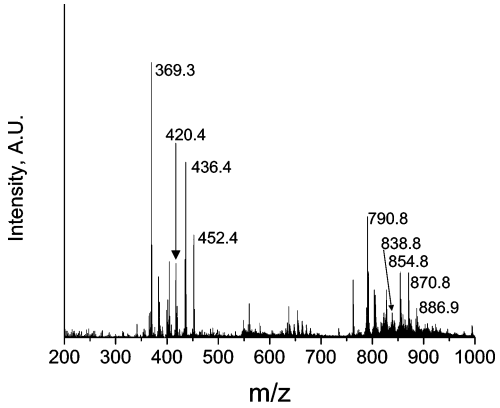

Figure 4. ESI-QTOF mass spectrum of an extract of the reacted cholesterol aerosol.

greater than 1000 *m*/*z*. Adjacent ions are separated by 1.0 u suggesting that no multiply charged ions are present. Many of the peaks observed in the positive ion mode are identified as MNH_4^+ (molecule plus a ammonium ion), as ion exchange with potassium (performed by adding KCl to the extract solution to give MK^+ in the mass spectrum) shifts each nominal mass by 21 u, the difference between NH_4^+ and K^+. Note that while negative ion analysis was performed, it yielded less information than that observed in the positive ion mode. For those ions that are not ammonium cationized, MH^+ ions are observed under the conditions used in this experiment despite the high concentrations of ammonium acetate or KCl. These are characterized by their odd mass signature. The broad groupings of singly charged ions in Figure 4 near 400 *m*/*z* are characteristic of oxygenated derivatives of cholesterol. It is known that the primary products from the reaction of cholesterol and ozone are likely to be vinyl hydroperoxides, bis-hemiacetals, ketones, and acids.[22,34] Ions at 420, 436, and 452 *m*/*z* (all M + NH_4^+) correspond to the addition of one, two, and three oxygens, respectively, to the cholesterol molecule. These products are the monomers from which the oligomeric molecules may form.[20,22,35−38] The monomer, dimer, and trimer (not shown in Figure 4) groupings are separated by about 450 u, which roughly corresponds to the median mass of a monomer unit. Within each grouping are smaller clusters of peaks. The clusters are separated by 14−18 u and are consistent with various combinations of monomer units with multiple sites of oxygen addition. The median m/z of each grouping corresponds to a whole number of monomers, suggesting that little monomer decomposition occurs during the formation of oligomers. Note that the relative ion intensities in Figure 4 do not necessarily indicate the relative product concentrations as molecular detection efficiencies can vary significantly in ESI.

While many studies have focused on the products of ozonolysis of cholesterol in participating and nonparticipating solvents,[21,26,39,40] most of these studies were done below room temperature. In contrast, the aerosol reactions were performed at ambient temperature. Thus, the first step in product characterization is identifying the first generation monomer reaction products from the aerosol phase reaction at ambient conditions using tandem MS (i.e., MSMS) in both the positive and the negative ion mode. Only the positive ion spectra are discussed below; the negative ion spectra did not provide any additional information other than to confirm the positive ion spectral interpretations.

Scheme 1 illustrates reaction mechanisms that could lead to the primary products observed in Figure 4. (While other reaction mechanisms and products may exist, Scheme 1 illustrates plausible reaction pathways and structures for the major ions observed.) This figure shows the representative oxygenated monomer building blocks as a result from the initial primary ozonide cleaving to form the intermediate Criegee zwitterion

SCHEME 1: Summary of the Mechanism of Cholesterol Ozonation That Leads to the Formation of Monomer Species[a]

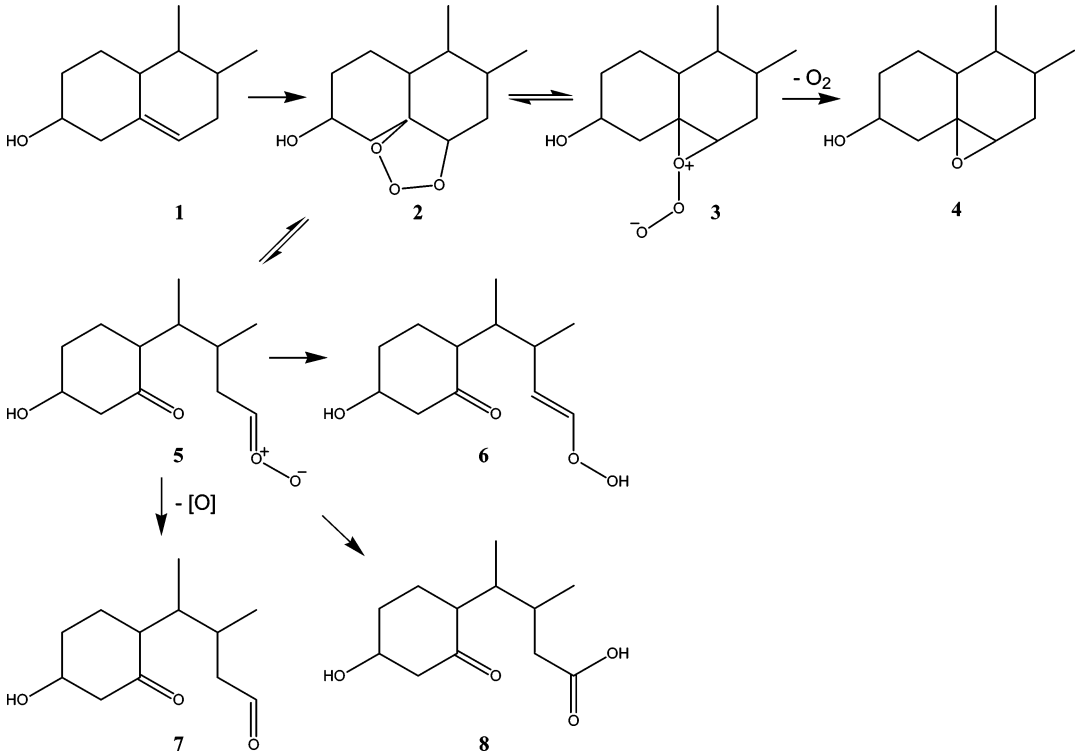

[a] Further mechanistic details are given in ref 22. The nonreactive portion of the cholesterol molecule has been omitted for clarity. See Figure 2 for the complete molecular structure.

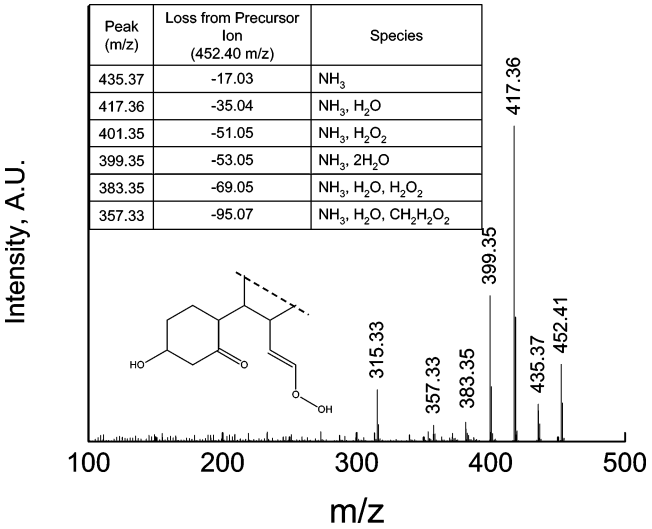

Figure 5. Product ion spectrum of the 452 *m*/*z* precursor. Note that only the reactive portion of the cholesterol molecule is shown, while the rest of the molecule is delineated by the dashed line. Hydrogen rearrangements and/or dehydrogenation reactions that accompany some fragmentations are not shown in the inset.

(**5**).[41] There are as many pathways as there are potential products, so only some routes are shown here. The zwitterion may isomerize, forming the partial cleavage product epoxide, **4**.[39,42] It can also isomerize, eject a hydroxyl radical, and form the dicarbonyl product **7**.[43,44] Alternatively, the vinyl hydroperoxide **6** may be generated.[42] The carbonyl oxide may form the secondary ozonide, which can thermally decompose, resulting in the acid-alcohol product **8**.[44] Other reaction pathways that lead to monomers and decomposition products are possible, but the ones just described appear to be operative in this case as described in the following section. Note that products **4**, **7**, and **6**/**8** correspond to the addition of 1, 2, and 3 oxygen atoms as indicated in Figure 4.

Verification of the proposed products in Scheme 1 was performed by tandem mass spectrometry. In this experiment, precursor ions are selected using the quadrupole mass selector, fragmented using collision-induced dissociation, and the product ions of the selected precursor are mass analyzed. In general, the product ion signal intensities from the precursors in Figure 4 were weak, although only moderate collision energies of 50−70 eV were required to achieve detectable signals. Figure 5 shows the product ion spectrum of the 452 *m*/*z* precursor ion, MNH_4^+, of the tri-oxygenated product, structure **6** or **8**. While structures **6** and **8** are both structures that lead to a product at this exact mass, others are possible.

The product ion spectrum of 452 *m*/*z*, shown in Figure 5, contains some ions that would be expected from structure **6** rather than **8**. Product ions consistent with structure **6** include 401 *m*/*z* (losses of ammonia and hydrogen peroxide), 383 *m*/*z* (dehydration of the molecular ion, most likely from the alcohol group, loss of ammonia and hydrogen peroxide), and 357 *m*/*z* (losses of methyl hydroperoxide, ammonia, and water). Note that the bond cleavages shown in the inset of Figure 5 do not include hydrogen rearrangements and/or dehydrogenation reactions that accompany many of these fragmentations. All have been observed previously for a similar product from cholesterol ozonolysis.[26] While structure **8** is very similar to structure **6**, it is not as consistent with the product ion spectrum in Figure 5. Structure **8** would be expected to give significant ion intensity at 391 *m*/*z* due to loss of CO_2, typical of acids. What is more, acids do not typically dehydrate upon collision-induced dissociation, although the dehydration products could arise from the alcohol functionality. What is surprising, however, is that no peak corresponds to loss of 28 u, consistent with a carbonyl moiety found in both structures.

SCHEME 2: Summary of the Mechanism of Cholesterol Ozonation That Leads to Dimer Products by Addition Across the Peroxidic Moiety[a]

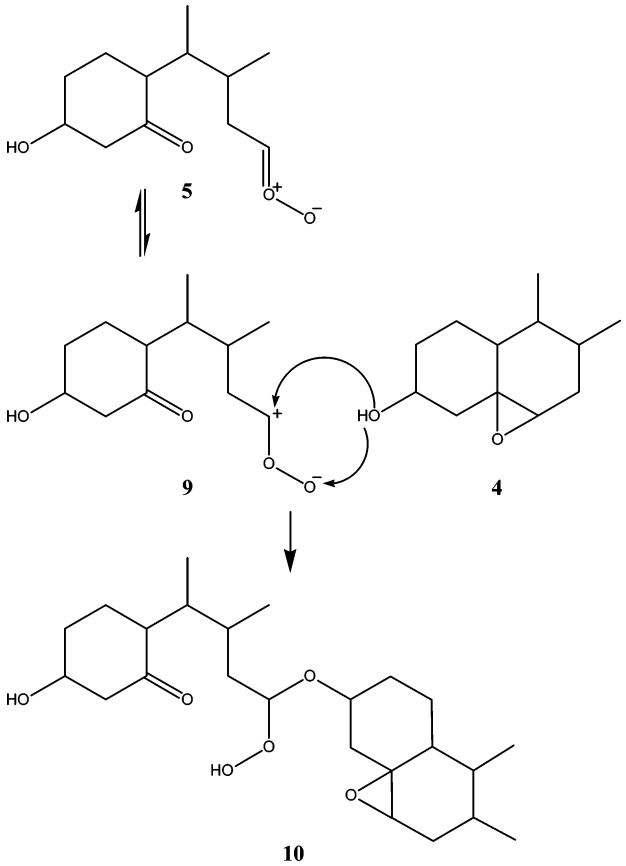

[a] Further mechanistic details are given in ref 22. The nonreactive portion of the cholesterol molecule has been omitted for clarity.

The consistency of Figure 5 (obtained from cholesterol particle ozonolysis) with products formed in solution was checked by reacting cholesterol with ozone in methylene chloride (a nonparticipating solvent) at room temperature.[21] The ESI-QTOF mass spectrum of this sample included numerous ions that corresponded to the aerosol phase spectrum. The product ion spectrum of the 452 *m*/*z* precursor from this sample contained all of the ions found in Figure 5, most notably 399, 383, and 357 *m*/*z* with intensities similar to those of the filter sample. It should be noted that while the compositions (product distribution, absolute concentration) of this sample solution and the solution used to obtain Figure 5 were not identical, similar CID spectra for the 452 *m*/*z* ion were obtained, which indicates that the same 452 *m*/*z* product ion structure was formed in the two cases, suggesting similar structures.

It has been known for some time that peroxidic oligomers result from alkene ozonolysis.[20] Scheme 2 outlines the probable mechanism for dimer formation in the aerosol phase. As in Scheme 1, the primary ozonide is cleaved and forms the Criegee intermediate zwitterion **5**. In Scheme 2, the zwitterion **5** reacts with an oxygenated cholesterol derivative **4**, which adds across the carbonyl oxide to form **10**, the acyl hydroperoxidic product. Note that if water were present, it would be expected to preferentially add across the carbonyl oxide, forming the

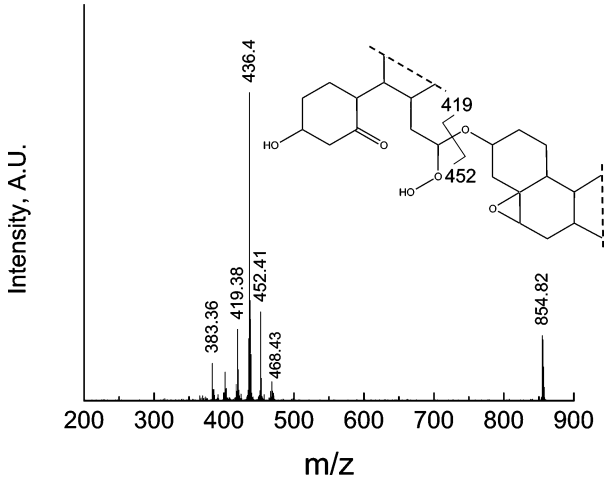

Figure 6. Product ion spectrum of the 854 *m*/*z* precursor. Only the reactive portion of the molecule is shown. Hydrogen rearrangements and/or dehydrogenation reactions that accompany some fragmentations are not shown in the inset.

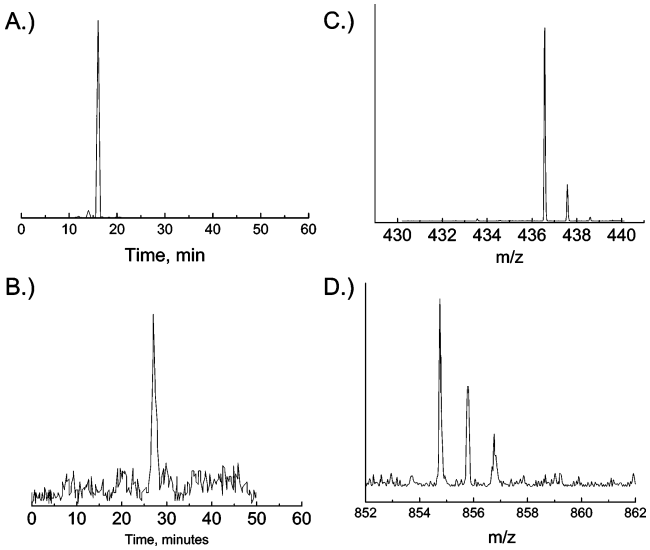

Figure 7. Selected ion chromatograms of (A) monomer reaction product at 436 *m*/*z* and (B) dimer reaction product at 854 *m*/*z*. Mass spectra at the peak of the chromatograms in (A) and (B) are shown in (C) and (D), respectively.

hydroxy hydroperoxide bis-hemiacetal.[26] This product was not observed under the reaction conditions used in this study. Thus, it appears that at low relative humidities, water does not play a significant role in product formation in the aerosol phase.

Figure 6 shows the product ion spectrum from 854 *m*/*z*. This precursor *m*/*z* corresponds to structure **10**, a dimer of **4** and **5**. Product ions in Figure 6 that are consistent with structure **10** include 452 *m*/*z* (cleavage at the peroxide bond), 436 *m*/*z* (cleavage α to the peroxide bond), and 419 *m*/*z* (436 − NH_3). Other products are observed that correspond to the combination of the Criegee zwitterion **5** with both cholesterol itself (**1**; 404 *m*/*z* in Figure 4) and the first generation products **6** (436 *m*/*z*) and **7** (452 *m*/*z*); all *m*/*z* values correspond to M + NH_4^+. The dimer products are observed at 838, 870, and 886 *m*/*z*, respectively (M + NH_4^+). MSMS of the 870 *m*/*z* product was similar to that of the 854 *m*/*z* product in that the major fragmentation was along the hemi-acetal moiety rather than the cholesterol backbone. The ion signals at 838 and 886 *m*/*z* were too small to obtain high-quality MSMS spectra. Note too, that other peaks appear in Figure 4 that correspond to products that have not been identified and may be the result of reaction schemes other than the one suggested here.

Of concern in these analyses is the formation of molecular clusters inside the ESI source. To confirm that the oligomers observed in this study were not ESI artifacts, samples were analyzed by LC−MS. It was found that the upper envelope of peaks that correspond to dimers eluted at different retention times than the monomer species (see Figure 7). In this case, the selected ion chromatogram at 436 *m*/*z* (M + NH_4^+) peaks at 15 min retention time. (Note that it is found in both the filter and the solution-phase samples.) However, the dimer peak at 854 *m*/*z* (2M + NH_4^+) elutes more than 10 min later, and no appreciable signal is observed at the same retention time as the monomer species. This indicates that the signal due to 854 *m*/*z* is due to a covalently bound species. However, cholesterol itself readily formed clusters (see the large peak at 790 *m*/*z* in Figure 4 that corresponds to 2M + NH_4^+ formed in the ESI source). In the tandem MS analysis of this ion, little if any collision energy and/or collision gas was needed for fragmentation, indicating that metastable decay was efficient and the precursor ion had a very low barrier to dissociation. The only product ions observed corresponded to the cholesterol monomer, which is expected for dissociation of a noncovalently bound cluster.

Trimer species were also observed (*m*/*z* range not shown in Figure 4). However, due to low signal intensity, MSMS analysis was not possible. It could be anticipated that the reaction sequence described in Scheme 2 would be effective in producing covalently bound oligomers with greater than two monomer units.

Atmospheric Implications. For typical ozone concentrations in air, a reaction probability of roughly 10^{-5} is required for a heterogeneous process to represent an important ozone sink.[45] Thus, reaction with cholesterol is not likely to be an important sink for ozone. For cholesterol that is emitted into the atmosphere, its lifetime will be on the order of days. This value implies that cholesterol can be used as a local source tracer for organic aerosol, but probably should not be used to determine regional sources of meat cooking operations.[7] It should be noted that reactive uptake could be modified by substrate effects. For example, cholesterol from meat cooking operations will likely coexist in particles containing other organic compounds such as fatty acids, which could modify the uptake mechanism. Also, meat cooking aerosol that is processed in the atmosphere will likely have enhanced deliquescent properties[46] that could modify cholesterol reactivity by increasing the particulate water content. Finally, this study provides another example of how organic oligomers can be prevalent in the aerosol phase.

Acknowledgment. Joy Ginter and Ann Snellinger are acknowledged for their assistance in ESI-MS analysis. Terrence Schull provided insight into organic reaction mechanisms. This research was supported by the National Science Foundation under grant number CHE-0098831.

References and Notes

(1) Schauer, J. J.; Rogge, W. F.; Hildemann, L. M.; Mazurek, M. A.; Cass, G. R.; Simoneit, B. R. T. *Atmos. Environ.* **1996**, *30*, 3837.

(2) Mazurek, M. A.; Simoneit, B. R. T.; Cass, G. R.; Gray, H. A. *Int. J. Environ. Anal. Chem.* **1987**, *29*, 119.

(3) Hawthorne, S. B.; Krieger, M. S.; Miller, D. J.; Mathiason, M. B. *Environ. Sci. Technol.* **1989**, *23*, 470.

(4) Hawthorne, S. B.; Miller, D. J.; Langenfeld, J. J.; Krieger, M. S. *Environ. Sci. Technol.* **1992**, *26*, 2251.

(5) Fraser, M. P.; Lakshamanan, K. *Environ. Sci. Technol.* **2000**, *34*, 4560.

(6) Simoneit, B. R. T.; Rushdi, A. I.; Bin Abas, M. R.; Didyk, B. M. *Environ. Sci. Technol.* **2003**, *37*, 16.
(7) Rogge, W. F.; Hildemann, L. M.; Mazurek, M. A.; Cass, G. R.; Simoneit, B. R. T. *Environ. Sci. Technol.* **1991**, *25*, 1112.
(8) Purvis, C. R.; McCrillis, R. C.; Kariher, P. H. *Environ. Sci. Technol.* **2000**, *34*, 1653.
(9) Hildemann, L. M.; Klinedinst, D. B.; Klouda, G. A.; Currie, L. A.; Cass, G. R. *Environ. Sci. Technol.* **1994**, *28*, 1565.
(10) Simoneit, B. R. T. *Int. J. Environ. Anal. Chem.* **1986**, *23*, 207.
(11) Benner, B. A., Jr.; Gordon, G. E.; Wise, S. A. *Environ. Sci. Technol.* **1989**, *23*, 1269.
(12) Paputa-Peck, M. C.; Marano, R. S.; Scheutzle, D.; Riley, T. L.; Hampton, C. V.; Prater, T. J.; Skewes, L. M.; Jensen, T. E.; Ruehle, P. H.; Bosch, L. C.; Duncan, W. P. *Anal. Chem.* **1983**, *55*, 1946.
(13) Later, D. W.; Andros, T. G.; Lee, M. L. *Anal. Chem.* **1983**, *55*, 2126.
(14) Bayona, J. M.; Markides, K. E.; Lee, M. L. *Environ. Sci. Technol.* **1988**, *22*, 1440.
(15) Stephanou, E. G.; Stratigakis, N. *Environ. Sci. Technol.* **1993**, *27*, 1403.
(16) Hildemann, L. M.; Mazurek, M. A.; Cass, G. R.; Simoneit, B. R. T. *Aerosol Sci. Technol.* **1994**, *20*, 303.
(17) Koeber, R.; Bayona, J. M.; Niessner, R. *Environ. Sci. Technol.* **1999**, *33*, 1552.
(18) Sauret, N.; Millet, M.; Herckes, P.; Mirabel, P.; Wortham, H. *Environ. Pollut.* **2000**, *110*, 243.
(19) Chien, C.-J.; Charles, M. J.; Sexton, K. G.; Jeffries, H. E. *Environ. Sci. Technol.* **1998**, *32*, 299.
(20) Greenwood, F. L.; Rubinstein, H. *J. Org. Chem.* **1967**, *32*, 3369.
(21) Jaworski, K.; Smith, L. L. *J. Org. Chem.* **1988**, *53*, 545.
(22) Bailey, P. S. *Ozonation in Organic Chemistry*, 1st ed.; Academic Press: New York, 1978.
(23) Oktem, B.; Tolocka, M. P.; Johnston, M. V. *Anal. Chem.* **2004**, *76*, 253.
(24) Liu, B. Y. H.; Ziemann, P. J.; Kittleson, D. B.; McMurry, P. H. *Aerosol Sci. Technol.* **1995**, *22*, 293.
(25) Liu, B. Y. H.; Ziemann, P. J.; Kittleson, D. B.; McMurry, P. H. *Aerosol Sci. Technol.* **1995**, *22*, 314.
(26) Pulfer, M. K.; Harrison, K.; Murphy, R. C. *J. Am. Soc. Mass Spectrom.* **2004**, *15*, 194.
(27) Morris, J. W.; Davidovits, P.; Jayne, J. T.; Jimenez, J. L.; Shi, Q.; Kolb, C. E.; Worsnop, D. R.; Barney, W. S.; Cass, G. R. *Geophys. Res. Lett.* **2002**, *29*, 1.
(28) Smith, G. D.; Woods, E.; DeForest, C. L.; Baer, T.; Miller, R. E. *J. Phys. Chem. A* **2002**, *106*, 8085.
(29) Tolocka, M. P.; Saul, T. D.; Johnston, M. V. *J. Phys. Chem. A* **2004**, *108*, 2659.
(30) McMurry, P. H.; Wang, X.; Park, K.; Ehara, K. *Aerosol Sci. Technol.* **2002**, *36*, 227.
(31) Rudich, Y. *Chem. Rev.* **2003**, *103*, 5097.
(32) Moise, M.; Rudich, Y. *J. Phys. Chem. A* **2002**, *106*, 6469.
(33) Vieceli, J.; Ma, O. L.; Tobias, D. J. *J. Phys. Chem. A* **2004**, *108*, 5806.
(34) Pulfer, M. K.; Murphy, R. C. *J. Biol. Chem.* **2004**, *279*, 26331.
(35) Antonovskii, V. L. *Kinet. Catal.* **2003**, *44*, 54.
(36) Tolocka, M. P.; Jang, M.; Ginter, J. M.; Cox, F. J.; Kamens, R.; Johnston, M. V. *Environ. Sci. Technol.* **2004**, *38*, 1428.
(37) Gao, S.; Keywood, M.; Ng, N. L.; Surratt, J.; Varutbangkul, V.; Bahreini, R.; Flagan, R. C.; Seinfeld, J. H. *J. Phys. Chem. A* **2004**, *108*, 10147.
(38) Barton, M.; Ebdon, J. R.; Foster, A. B.; Rimmer, S. *J. Org. Chem.* **2004**, *69*, 6967.
(39) Gumulka, J.; Smith, L. L. *J. Am. Chem. Soc.* **1983**, *105*, 1972.
(40) Paryzek, Z.; Rychlewska, U. *J. Chem. Soc., Perkin Trans.* **1997**, 2313.
(41) Criegee, R. *Angew. Chem., Int. Ed. Engl.* **1975**, *14*, 745.
(42) Martinez, R. I.; Herron, J. T.; Huie, R. E. *J. Am. Chem. Soc.* **1981**, *103*, 3807.
(43) Griesbaum, K.; Hilss, M.; Bosch, J. *Tetrahedron* **1996**, *52*, 14813.
(44) Jang, M.; Kamens, R. M. *Atmos. Environ.* **1999**, *33*, 459.
(45) Dentener, F. J.; Carmichael, G. R.; Zhang, Y.; Lelieveld, J.; Crutzen, P. J. *J. Geophys. Res.* **1996**, *101*, 22.
(46) Asad, A.; Mmereki, B. T.; Donaldson, D. J. *Atmos. Chem. Phys. Discuss.* **2004**, *4*, 4019.